Inferential framework for autonomous cryogenic loading operations

Dmitry G Luchinskiy[1], Michael Khasin[2], Dogan Timucin[3], Jarred Sass[4], Jose Perotti[5], Barbara Brown[6]

[1,2] *SGT, Inc., Greenbelt, MD, USA*
dmitry.g.luchinsky@nasa.gov
michael.khasin@nasa.gov

[3] *NASA Ames Research Center, Moffett Field, CA, 94035, USA*
dogan.timucin@nasa.gov

[4,5,6] *Kennedy Space Center, Kennedy Space Center, FL, 32899, USA*
jose.m.perotti@nasa.gov
jared.p.sass@nasa.gov
barbara.l.brown@nasa.gov

ABSTRACT

We address problem of autonomous cryogenic management of loading operations on the ground and in space. As a step towards solution of this problem we develop a probabilistic framework for inferring correlations parameters of two-fluid cryogenic flow. The simulation of two-phase cryogenic flow is performed using nearly-implicit scheme. A concise set of cryogenic correlations is introduced. The proposed approach is applied to an analysis of the cryogenic flow in experimental Propellant Loading System built at NASA KSC. An efficient simultaneous optimization of a large number of model parameters is demonstrated and a good agreement with the experimental data is obtained.

1. INTRODUCTION

NASA program of advanced cryogenic loading operations is focused on development of technologies enabling effective space exploration (Chato, 2008; Notardonato, 2012; Konishi & Mudawar, 2015a). These technologies require models that can recognize and predict cryogenic fluid regimes without human interaction. The accuracy of these predictions depend largely on the functional form and parameterization of correlations for the flow patterns, pressure losses, and the heat transfer in cryogenic fluids. However, knowledge of these correlations remains limited and their learning present significant challenge to scientists and engineers (Tong & Tang, 1997; Faghri & Zhang, 2006; Ghiaasiaan, 2007; Konishi & Mudawar, 2015b) This problem becomes even more challenging for applications in micro-gravity (S. R. Darr et al., 2016a, 2016b).

Research conducted to address this and other critical issues of space exploration resulted in a number of important achievements, see e.g. (Konishi & Mudawar, 2015a; S. R. Darr et al., 2015; Hartwig & Vera, 2015; Hedayatpour, Antar, & Kawaji, 1990; Kawaji, 1996; A. Majumdar & Steadman, 2003; A. K. Majumdar & Ravindran, 2010; Yuan, Ji, & Chung, 2007, 2009; Chung & Yuan, 2015; S. Darr et al., 2016; S. R. Darr et al., 2016a, 2016b) and references therein. Specifically, a number of optimization techniques have become available for analysis of the model parameters and data correlations (Cullimore, 1998).

However, small time steps and instabilities of numerical schemes impose substantial limitations on the speed of the two-fluid cryogenic codes and possibility of their on-line applications in autonomous systems. As a result accurate predictions of transient cryogenic flows and optimization of the parameters of cryogenic systems remain a challenge (Hartwig & Vera, 2015; Cullimore, 1998; Konishi & Mudawar, 2015a; S. R. Darr et al., 2015).

Here we report on progress in development of probabilistic framework capable of efficient multi-parametric inference of cryogenic correlations and accurate predictions of experimental time-series data.

The paper is organized as follows. In the following section we briefly describe model equations and method of their integration. In Sec. 3 we discuss correlation relations for two-phase cryogenic fluid. In Sec. 4 we introduce probabilistic frame-

work for multi-parametric inference of the model parameters. An application of the inferential framework to the analysis of cryogenic flow in experimental Propellant Loading System is discussed in Sec. 5. Finally, in Conclusions we summarize the obtained results and discuss future applications.

2. MODEL

2.1. Model equations

The system is modeled using six conservation equations for gas/vapor and liquid phases in a set of control volumes (D. G. Luchinsky, Smelyanskiy, & Brown, 2014a, 2014c, 2014b; D. G. Luchinsky et al., 2016), see also (Luchinskiy, Ponizovskaya-Devine, Hafiychuk, et al., 2015; D. G. Luchinsky et al., 2015). The set of equations can be written as following

$$\begin{aligned}\frac{\partial}{\partial t}\left[\begin{array}{c}\alpha\rho\\ \alpha\rho u\\ \alpha\rho e\end{array}\right]_j+\frac{\partial}{\partial t}\left[\begin{array}{c}\alpha\rho u\\ \alpha\rho u^2\\ \alpha\rho e u\end{array}\right]_j\\ =\left[\begin{array}{c}0\\ 0\\ p\left(s\,\alpha_{,t}-(\alpha u)_{,x}\right)\end{array}\right]_j\\ +\left[\begin{array}{c}s_j\,\Gamma\\ \alpha\rho z_{,x}-\tau_w l_w-\tau_i l_i+\Gamma u_i\\ \dot{q}_w\frac{l_w}{A}+\dot{q}_i\frac{l_i}{A}+\Gamma h_i\end{array}\right]_j\end{aligned} \tag{1}$$

Here j takes values g for the gas and l for the liquid and dynamical variables in this system are: void fraction α (volume conservation requires $\alpha_g+\alpha_l=1$), pressure p, phasic densities $\rho_{g(l)}$, velocities $u_{g(l)}$, and thermal energies $e_{g(l)}$, s_j is negative sign for the liquid and positive for the gas. The system (1) is closed by constitutive relations and equations of states implemented in the form of tables. The values of heat ($\dot{q}$) and mass (Γ) fluxes at the wall and interface (subscripts w and i) are given by correlation relations.

The system (1) is coupled to the energy conservation equation for the pipe walls

$$\begin{aligned}\rho_w c_w d_w\tfrac{\partial T_w}{\partial t}=h_{wg}\left(T_g-T_w\right)\\ +h_{wl}\left(T_l-T_w\right)+h_{amb}\left(T_{amb}-T_w\right).\end{aligned} \tag{2}$$

Here T_w is the pipe wall temperature, ρ_w, c_w, and d_w are density, specific heat, and thickness of the pipe wall, h is the heat transfer coefficient corresponding to the ambient (h_{amb}) and internal heat flowing to the wall from the gas (h_{wg}) and liquid (h_{wl}) phases.

The total mass transfer Γ_g in equations (1) is the sum of the mass transfer at the wall (w) and at the interface (i)

$$\Gamma_g=\Gamma_{wg}+\Gamma_{ig},$$

where

$$\Gamma_{wg}=\frac{\dot{q}_{wl}}{H_g^*-H_l^*};\qquad \Gamma_{ig}=\frac{\dot{q}_{li}+\dot{q}_{gi}}{H_g^*-H_l^*};$$

and

$$H_g^*-H_l^*=\left\{\begin{array}{ll}H_{g,s}-H_l, & \Gamma>0\\ H_g-H_{l,s}, & \Gamma<0\end{array}\right..$$

The heat fluxes at the wall and at the interface are defined as follows

$$\begin{array}{ll}\dot{q}_{wg}=h_{wg}\left(T_w-T_g\right); & \dot{q}_{ig}=h_{ig}\left(T_{l,s}-T_g\right);\\ \dot{q}_{wl}=h_{wl}\left(T_w-T_l\right); & \dot{q}_{il}=h_{il}\left(T_{l,s}-T_l\right).\end{array}$$

Here $T_{l,s}$ is the saturation temperature of the liquid.

2.2. Algorithm

The integration of the model (1) - (2) was performed in two steps following closely the nearly-implicit method described in RELAP5-3D (RELAP5-3D-I, 2012), see (D. G. Luchinsky et al., 2014c; Luchinskiy, Ponizovskaya-Devine, Hafiychuk, et al., 2015) for the details. The first step of the algorithm can be briefly summarized as follows: (i) Solve expanded equation with respect to pressure in terms of new velocities; (ii) Solve momenta equations written in the form of block tridiagonal matrix for the new velocities; (iii) Find new pressure; (iv) Find provisional values for energies and void fractions using expanded equations; (v) Find provisional values of mass fluxes and heat transfer coefficients using provisional values of temperatures obtained.

At the second step new values of the densities, void fractions, and energies are found by solving the unexpanded conservation equations for the phasic masses and energies using provisional values for the heat and mass fluxes in source terms. The solution is reduced to independent solution of four tridiagonal matrices. The values of pressure and velocities in these matrices are taken at the new time step.

The resulting computational scheme is efficient and fast and can integrate 1000 sec of real time chilldown in a few seconds of computational time. For a model consisting of N control volumes it involves inversion of N 4×4 matrices, solution of $2\times(N-1)$ tree-block-diagonal matrix equation, solution of four $N\times N$ tridiagonal matrix equations, and $N\times m$ explicit computations.

The mitigation of known stability issues of this algorithm is discussed in (D. G. Luchinsky et al., 2014a, 2014c, 2014b, 2016; Luchinskiy, Ponizovskaya-Devine, Hafiychuk, et al., 2015; D. G. Luchinsky et al., 2015)

3. CONSTITUTIVE RELATIONS

The model equations introduced above have to be closed using the equations of state and the constitutive relations. The equations of state can be included into the model in the

form of NIST tables (Lemmon, Huber, & McLinden, 2013; D. G. Luchinsky et al., 2014c). Functional and parametric form of constitutive relations, on the other hand, represent one of the main source of uncertainties in the model. In this work we use constitutive relations (D. G. Luchinsky et al., 2016) based on the recognition of the flow boiling regimes and for each regime we define interphase friction, the coefficient of virtual mass, wall friction, wall heat transfer, interphase heat and mass transfer.

At each time step the boundaries between flow boiling regimes are determined first, then the flow correlations are defined for each flow regime.

The boundaries between flow regimes are estimated using simplified Wojtan et al (Wojtan, Ursenbacher, & Thome, 2005) map. The map was simplified in two ways. First we used only three transition boundaries. Next, we estimated the location of these boundaries in the coordinates of mass flow rate ($\dot{m}$) and vapor quality (χ) using original expressions. Finally, we approximated the location of these boundaries using low-dimensional polynomials and used polynomial coefficients as fitting parameters.

The rationale behind approximate description of the boundaries of flow regimes is twofold. It is known (Jackson, 2006) that Wojtan maps can only be considered as an approximation to the flow regimes for cryogenic fluids. In the experiments performed at KSC the flow regimes were not established experimentally and therefore cannot be validated.

The following transitions between flow regimes were included into correlations: (i) Stratified-Wavy-to-stratified transition; (ii) Stratified-Wavy-to-annular-intermittent transition; and (iii) Dryout transition.

3.1. Heat and mass transfer

In the current work we are interested in relatively low mass fluxes, $G < 600kg/m^2/s$. In this limit correlations for the heat flux are often based on the multiplicative or additive corrections to the values obtained for pool boiling (Franchello, 1993; Seader, Miller, , & Kalvinskas, 1965; Griffith, 1957; Zuber & Tribus, 1958; Kutateladze, 1959). The following heat transfer mechanisms are included in the analysis: (i) convection, (ii) nucleate boiling, (iii) transition boiling, (iv) film boiling, and (v) transition to dryout regime.

3.1.1. Convective Heat Transfer

Convective heat transfer in horizontal pipes distinguishes four flow regimes: forced laminar, forced turbulent, natural laminar, and natural turbulent convection. The corresponding correlations for the convective heat transfer can be taken in the form e.g. (TRACE-V5.0, 2007; RELAP5-3D-IV, 2012; Nellis & Klein, 2009; Holman, 1989)

$$h_{cb} = \frac{\kappa}{D_h} \begin{cases} 4.36, & \text{Forced-Laminar;} \\ 0.023 \cdot Re^{0.8} Pr^{0.4}, & \text{Forced-Turbulent;} \\ 0.1 \cdot (Gr \cdot Pr)^{1/3}, & \text{Natural-Laminar;} \\ 0.59 \cdot (Gr \cdot Pr)^{1/4}, & \text{Natural-Turbulent.} \end{cases} \quad (3)$$

Here $Pr = \frac{\mu C_p}{\kappa}$ and $Gr = \frac{\rho^2 g \beta_T (T_w - T_{l(g)}) D^3}{\mu^2}$ are Prandtl and Grashof numbers respectively, β_T is the coefficient of thermal expansion, and D_h is the hydraulic diameter. To guarantee a smooth transition between various regimes the maximum value of h_{cb} is taken as the value for the convective heat transfer.

We note that convective heat transfer in the stratified flow does not significantly affect the chilldown process, because the fluid temperature in this regime is close to (or lower than) saturation temperature T_s. The first critical temperature that defines the shape of the boiling curve and influences the chilldown corresponds to the onset of nucleation boiling T_{onb}.

3.1.2. Onset of nucleate boiling

The correlations for temperature T_{onb} and the corresponding heat flux $\dot{q}_{onb}$ for onset of nucleate boiling can be written (Sato & Matsumura, 1964; Frost & Dzakowic, 1967; Ghiaasiaan, 2007; Huang, 2009) as

$$T_{onb} = T_s + F\left(1 + \sqrt{1 + \frac{2\Delta T_{sub}}{F}}\right), \quad (4)$$

$$\dot{q}_{onb} = \frac{B}{Pr^2}\,\Delta T_{sat}^2 = h_{cb}(T_{onb} - T_l) \quad (5)$$

where $B = \frac{\rho_g h_{lg} \kappa_l}{8\sigma T_s}$, $F = \frac{h_{cb} Pr_l^2}{2B}$, $\Delta T_{sat} = T_{onb} - T_s$ is the wall superheat, and $\Delta T_{sub} = T_s - T_l$ is liquid subcooling temperature. The convective heat transfer coefficient is given by (3).

When the wall temperature is increased the heat flux to the wall may increase by more than an order of magnitude until the heat flux approaches its critical value $\dot{q}_{chf}$.

3.1.3. Critical heat flux

The values of critical heat flux $\dot{q}_{chf}$ and the corresponding critical wall superheat T_{chf} are crucial for predicting chilldown and dryout phenomena in non-equilibriums flows. In nuclear reactor codes. (RELAP5-3D-IV, 2012; TRACE-V5.0, 2007) these values are determined using look-up tables based on extensive experimental measurements obtained under various flow conditions. For cryogenic fluids experimental data remain sparse and values of $\dot{q}_{chf}$ and T_{chf} are often estimated using mechanistic models (Tong & Tang, 1997; Ghiaasiaan, 2007; Seader et al., 1965; Crowley & Izenson, 1989; Konishi & Mudawar, 2015b).

The temperature T_{chf} for the critical heat flux was estimated in this work using approach proposed by Theler (Theler & Freis, 2011)

$$T_{chf} = \frac{T_s}{1 - \frac{T_s R_g}{h_{lg}} log(2k_g + 1)}, \quad (6)$$

where k_g is the isoentropic expansion factor that for ideal diatomic gases is 7/2 and R_g is the specific gas constant.

In boiling flows critical heat flux corrections have to take into account the dependence of the heat flux on the void fraction, velocity, and sub-cooling of the flow. In this work we used correlations proposed by Griffith et all for cryogenic flows (Franchello, 1993; Seader et al., 1965)

$$\begin{aligned} \dot{q}_{chf} &= \dot{q}_{chf,0}(\alpha_{cr} - \alpha)\left(1 + a_1\left(\frac{\rho_l c_l \Delta T_{sub}}{\rho_g h_{lg}}\right)\right. \quad (7) \\ &\left. + a_2 Re_l + a_3\left(\frac{Re_l \rho_l c_l \Delta T_{sub}}{\rho_g h_{lg}}\right)^{1/2}\right), \end{aligned}$$

where α_{cr} is the critical value of the void fraction and a_i are constants, e.g. $a_1 = 0.0144$, $a_2 = 10^{-6}$, $a_3 = 0.5 \times 10^{-3}$ (Griffith, 1957), and $\alpha_{cr} = 0.96$ (Franchello, 1993) for water.

The term $\dot{q}_{chf,0}$ in the eq. (7) corresponds to the pool boiling correlations, which were estimated in the present work using Zuber (Zuber & Tribus, 1958) correlations

$$\dot{q}_{chf,0} = \frac{\pi}{24} h_{lg} \rho_g \left(\frac{\sigma g(\rho_l - \rho_g)}{\rho_g^2}\right)^{1/4} \left(\frac{\rho_l}{\rho_l + \rho_g}\right)^{1/2}. \quad (8)$$

In numerical tests, we often used a simplified expression for eq. (7), cf (Franchello, 1993; Iloeje, Plummer, Rohsenow, & Griffith, 1982)

$$\dot{q}_{chf} = \dot{q}_{chf,0} \cdot a_1 \cdot (\alpha_{cr} - \alpha)^{a_2}(1 + a_3 G^{a_5}), \quad (9)$$

where typical values of parameters used in simulations are a_1=1.0, α_{cr}=0.96, a_2=2.0, a_3=0.16, and a_4=0.2.

When wall superheat exceeds $\Delta T_{chf} = T_{chf} - T_s$, the transition boiling begins and the heat flux to the wall decreases sharply as a function of the wall temperature until the latter reaches minimum film boiling temperature T_{mfb}.

3.1.4. Minimum film boiling

In the film boiling regime the fluid flow is completely separated from the wall by the vapor film. The minimum value of the wall superheat $\Delta T_{mfb} = T_{mfb} - T_s$ corresponding to this regime was estimated by Berenson as (Carbajo, 1985; Berenson, 1961)

$$\begin{aligned} \Delta T_{mfb,0} = 0.127 \frac{\rho_g h_{lg}}{\kappa_g} \times \\ \left[\frac{g(\rho_l - \rho_g)}{\rho_l + \rho_g}\right]^{2/3} \left[\frac{\sigma}{g(\rho_l - \rho_g)}\right]^{1/2} \left[\frac{\mu_g}{(\rho_l - \rho_g)}\right]^{1/3} \quad (10) \end{aligned}$$

Iloeje (Franchello, 1993; Iloeje et al., 1982) has corrected Berenson equation to take into account the dependence of the ΔT_{mfb} on the quality and mass flux of the boiling flows in the form

$$\Delta T_{mfb} = c_1 \Delta T_{mfb,0}(1 - c_2 X_e^{c_3})(1 + c_4 G^{c_5}), \quad (11)$$

where X_e is the equilibrium quality, G is liquid mass flux and a_i are constants, e.g. $a_1 = 0.0144$, $a_2 = 10^{-6}$, $a_3 = 0.5 \times 10^{-3}$ (Griffith, 1957), and $\alpha_{cr} = 0.96$ (Franchello, 1993) for water.

The heat flux in the film boiling flow can be chosen following e.g. recommendations of Groeneveld and Rousseau (Groeneveld & Rousseau, 1983). In this work the heat flux to the wall in the film boiling regime was taken in the form of Bromley correlations

$$h_{br} = C \cdot \left[\frac{g \rho_g \kappa_g^2 (\rho_l - \rho_g) \tilde{h}_{lg} c_{pg}}{D(T_w - T_{spt}) Pr_g}\right]^{0.25}, \quad (12)$$

corrected using Iloeje-type correlations (Franchello, 1993; Iloeje et al., 1982)

$$h_{fb} = c_1 h_{br}(1 - c_2 X_e^{c_3})(1 + c_4 G^{c_5}) \quad (13)$$

Typical values of the parameters used in simulations are the following: (i) $c_1 = 2.0$; (ii) $c_2 = 1.04$; (iii) $c_3 = 2.0$; (iv) $c_4 = 0.2$; (v) $c_5 = 0.1$.

The minimum film boiling heat flux can now be defined as

$$\dot{q}_{mfb} = h_{fb} \Delta T_{mfb}. \quad (14)$$

To complete the discussion of the boiling heat transfer we notice that in the region of single phase gas flow the heat transfer is given by equations (3) with appropriately modified parameters. Transition to the single phase heat transfer is initiated when dryout transition is detected.

Further details of the constitutive relations, including pressure drop correlations, will be provided elsewhere, see e.g. (D. G. Luchinsky et al., 2016; D. Luchinsky, Khasin, Timucin, Sass, & Brown, 2016).

3.2. Uncertainties

Traditionally, the choice of the functional form of the correlations was the major source of uncertainty in cryogenic flow simulations. There have been literally hundreds of various modifications proposed for the flow boiling correla-

tions (Nellis & Klein, 2009; Shahs, 2006) and the corresponding functional space is continuously expanding (S. R. Darr et al., 2015; Kim & Mudawar, 2014; Konishi & Mudawar, 2015a).

In addition, the development of correlations rely on assumptions that can be viewed only as approximations. Furthermore, these approximations usually do not take into account surface wettability, pipe curvature, sub-cooling, and surface orientation.

At the fundamental level the uncertainties in two-fluid modeling stem from the fact that the interface between two phases is continuously fluctuating and neither location nor the shape of the interface can be resolved by the model. The intensity of these fluctuations is especially significant during chilldown, when liquid and vapor phases coexist under strongly non-equilibrium conditions, see e.g. (Yuan et al., 2007).

Accordingly, most of the parameters in the correlations discussed above should be considered as unknown fitting parameters of the problem. Their relative importance to the system dynamics is also unknown. And a general probabilistic framework is required to establish distribution of these parameters using available databases of cryogenic flows.

4. INFERENTIAL FRAMEWORK

4.1. Probabilistic approach

The approach to the solution of the inference problem adopted in this work is based on probabilistic Bayesian method (Ghahramani, 2015). Using this technique one can (Ghahramani, 2015) estimate the conditional probability of unknown model parameters θ

$$P(\theta|D,m) = \frac{P(D|\theta,m)P(\theta|m)}{P(D|m)}, \tag{15}$$

compare different models m

$$P(D|m) = \frac{P(m|D)P(m)}{P(D)} \tag{16}$$

and forecast system response D_n to untested experimental conditions

$$P(D_n|D,m) = \int P(D_n|\theta,D,m)P(\theta|D,m)d\theta. \tag{17}$$

In the equations above $P(D|\theta,m)$ is the likelihood of parameters θ in model m. In a typical step of parameter inference within Bayesian probabilistic framework one has to guess or estimate the prior probability of θ $P(\theta|m)$ and to obtained the improved posterior probability of θ $P(\theta|D,m)$ using available time-series data D.

There are two important advantages of this approach. First is the method's ability to select simpler models over more complex models. Second is the ability to chose model, which is flexible enough to resolve the complexity of the experimentally observed system dynamics.

4.2. State Space Model

To perform parameter estimation the equations (1) - (2) are integrated over the length of control volumes (D. G. Luchinsky et al., 2014c; RELAP5-3D-I, 2012). The result of integration at one time step is formally represented in a standard form of discrete time state space model (SSM)

$$\begin{aligned} x_{t+1} &= f(x_t,c) + \varepsilon_t, \\ y_t &= g(x_t,b) + \chi_t. \end{aligned} \tag{18}$$

Here x_t is a set of the main dynamical variables of the system $\{\rho_g, \rho_l, T_g,\ \ T_l, u_g, u_l, p, \alpha, T_w\}_t^L$ averaged over corresponding control volume at time instant t and c is the set of the model parameters.

The observations y_t in the SSM are related to the unobserved states via nonlinear function $g(x_t,b)$. ε_t and χ_t in equations (18) are independent identically distributed sources of Gaussian noise.

The simultaneous parameter and state estimations in nonlinear system (18) can be performed using a number of techniques, see e.g. (Ghahramani, 2015; Smelyanskiy, Luchinsky, Millonas, & McClintock, 2009; Duggento, Luchinsky, Smelyanskiy, & McClintock, 2009). Here, to simplify the problem we assume that measurement noise can be neglected and that pressure $\hat{p}$ and fluid temperature $\hat{T}_f$ can be measured directly in the experiment.

In the simplest case of general importance the problem was reduced to the curve fitting problem, cf (Cullimore, 1998), which was solved using global search algorithms available in

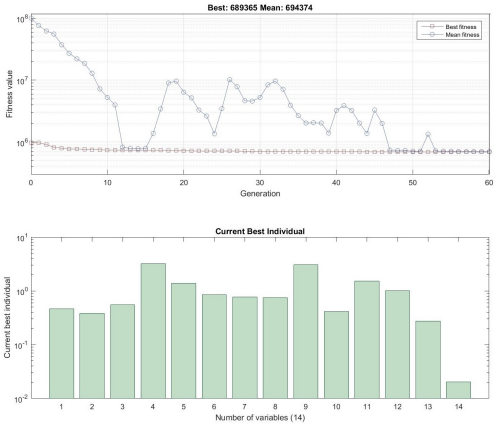

Figure 1. (a) Convergence of the genetic algorithm for simultaneous optimization of 14 model parameters. (b) Best values of the model parameters.

MATLAB optimization toolbox including genetic algorithm, pattern search, simulated annealing, and particle swarm.

An example of convergence is shown in Fig. 1. In this example the genetic algorithm was used for simultaneous optimization over 14 model parameters including characteristic time of the heat transfer to the wall, scaling coefficients for the mass transfer at the interface and at the wetted wall, for the film boiling heat transfer, for the dependence of the critical heat flux on the void fraction, for the heat transfer coefficients on both sides of liquid vapor interface, for the heat transfer to the dry wall, for the temperatures of the critical heat flux and minimum film boiling, exponent of the Reynolds number in the Ditus-Boetler at the dry wall, and parameters of the transition boundary to the dispersed flow regime.

To enforce the convergence an extensive preprocessing was used including sensitivity analysis of the model with respect to the full set of parameters, selection of a subset of the most sensitive parameters for each flow regime, and simplified direct search for initial estimations of sub-optimal values of the selected model parameters. Some further details of the approach can be found in (D. Luchinsky et al., 2016).

Below we provide an example of application of this approach to the analysis of chilldown in cryogenic horizontal line.

5. APPLICATION TO THE ANALYSIS OF THE CRYOGENIC LOADING SYSTEM

The time-series data analyzed in this work were obtained at the Simulated Propellant Loading System (SPLS) built at NASA KSC (Johnson, Notardonato, Currin, & Orozco-Smith, 2012).

5.1. SPLS

The SPLS line includes storage (ST) and vehicle (VT) tanks connected via cryogenic transfer line that has a number of in-line (CV) and bleed (BV) valves that control the flow. The

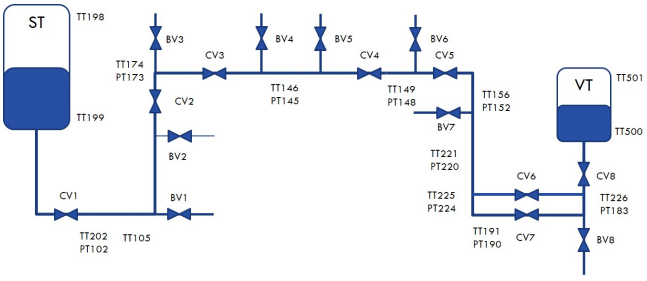

Figure 2. Sketch of the cryogenic transfer line built at KSC. It includes storage tank (ST) and vehicle tank (VT); the in-line control valves: CV1 through CV8; remotely controlled bleed valves: BV1 through BV8; ten in-line temperature sensors (TT) and 9 in-line pressure sensors (PT).

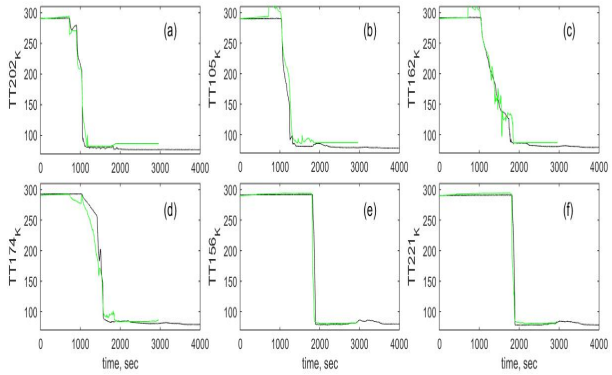

Figure 3. Model predictions (green lines) for the fluid temperature are shown in comparison with the experimental time-traces (black lines) at 6 different locations along the transfer line.

flow conditions are monitored using a set of pressure (PT) and temperature (TT) sensors. The sketch of the transfer line indicating the locations of the control valves and sensors is shown in the Fig. 2. The typical chilldown sequence measured by temperature sensors is illustrated in Fig. 3. The chilldown begins at ∼800 sec by opening the valve CV1 (note, that the initial time is chosen arbitrary). At this time all other valves remain closed and after a small temperature drop partial recovery of the temperature measured by sensor TT202 can be observed in Fig. 3(a).

Approximately ∼270 sec later the valves CV2 and BD 1, 2, and 3 are opened allowing liquid nitrogen to flow down through the system up to the location of the valve CV3. The cooling of the fluid in the pipes can be detected at this stage at temperature sensors TT202 though TT774. The chilldown of the first part of the transfer line is accomplished ∼1000 sec from the chilldown initiation, when the temperature sensor TT74 indicates the presence of the liquid nitrogen.

The final stage of chilldown begins at ∼2000 sec, when valve CV3 is opened and nitrogen is allowed to flow through the whole system. The chilldown of the second part of the transfer line can be observed at the sensors TT146 through TT226. The chilldown is completed when sensor TT226 indicates the presence of the liquid nitrogen.

The comparison of the model predictions (green lines in the Fig. 3) with the experimental time traces (black lines) shows that the model can quite accurately reproduce all three stages of the chilldown. We note that the model integration is fast. The integration of nearly 3000 sec of real time shown in the figures takes ∼10 seconds on laptop.

A good agreement between model predictions and experimental time-series data was achieved using a sequence of steps as will be discussed in more details below.

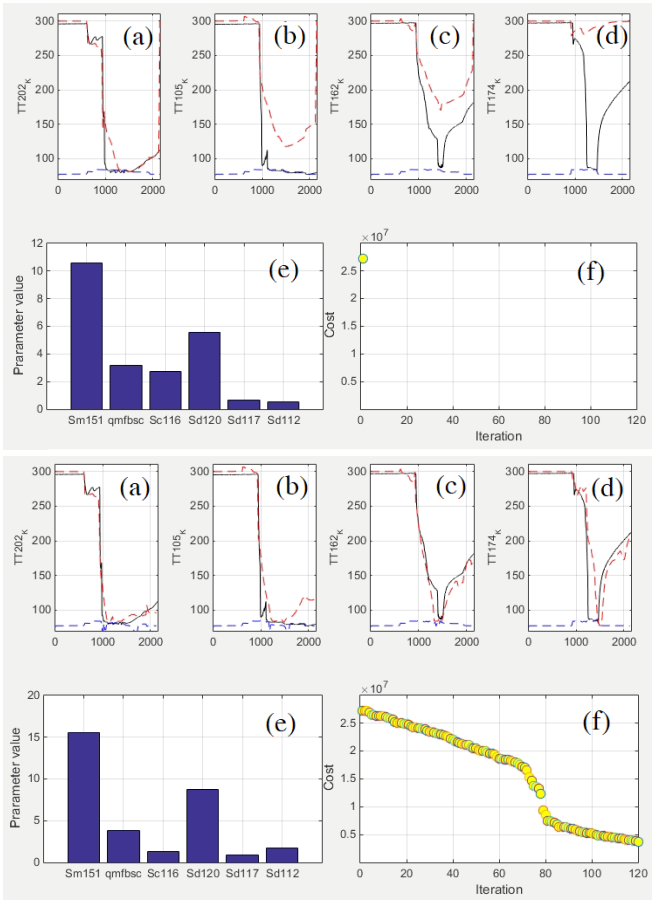

Figure 4. The simplified direct search algorithm: convergence of the model predictions (red dashed lines) towards experimental data (solid black lines) for gas temperature measured at four sensors: (a) TT202, (b) TT105, (c) TT162, and (d) TT174. The search is performed for 6 parameters of the SPLS model shown in figure (e). The cost function is shown in figure (f). (top) Initial state. (bottom) Final state.

5.2. Optimization of the SPLS parameters

The initialization and the update of the parameter distributions involves the following steps: (i) choice of the model parameters; (ii) definition of the objective function; (iii) analysis of the initial parameter's distributions using sensitivity study; (iv) estimation of sub-optimal parameter values using simplified direct search; (v) global search for the optimal values of the model parameters; and (vi) estimation of the variance of the optimized parameters.

There are about 98 parameters in the present model of the SPLS. Approximately half of these parameters correspond to the correlation relations. The remaining parameters describe valve coefficients, minor losses and leaks of the system components. Each parameter is tagged. Any number of parameters can be selected for optimization by listing corresponding tags in arbitrary order.

The cost function has the form of the sum of square errors on discrete time $t_n = \{t_0, ..., t_N\}$, cf. (Cullimore, 1998)

$$S(\mathbf{c}) = \sum_{n=0}^{N} \sum_{k=1}^{K} \left[\eta_{T_f} \left(T^k_{f,n}(\mathbf{c}) - \hat{T}^k_{f,n} \right)^2 + \eta_p \left(p^k_n(\mathbf{c}) - \hat{p}^k_n \right)^2 \right], \tag{19}$$

where η_i are weighting coefficients, $T^k_{f,n}(\mathbf{c})$ and $p^k_{f,n}(\mathbf{c})$ are predicted by the model fluid temperature and pressure at k-th location and n-th instant of time, pressure and temperature with the hat correspond to the measured time-series data, index k runs through different locations of the sensors.

The sensitivity study reveal ∼30 sensitive model parameters and subsequent optimization was focused on the analysis of this subset of parameters.

The optimization is performed in two steps. At the first step we apply simplified direct search algorithm: (i) the parameter space is discretized on a regular multi-dimensional grid; (ii) parameters are optimized one at a time using 1D search; (iii) the resulting optimal value of the given parameter is used in subsequent searchers; (iv) once the algorithm scanned through all the parameters the order of parameters is changed and the search is repeated. It was found that this step is essential to speed up the convergence and to find global minimum.

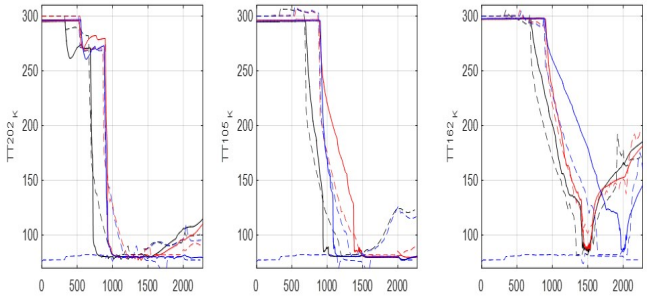

Figure 5. Comparison of the model predictions for the temperature time-series data (colored dashed lines) with the experimental results (colored solid lines) for the different openings of the valve cv112: (i) 15% blue line; (ii) 25% black line (nominal); (iii) 40% red line.

The convergence of the algorithm is illustrated in the Fig. 4 for simultaneous optimization of 6 parameters, which are scaling factors for the flow coefficients of the valves: Sm151 - input valve CV1; Sc116 for inline valve CV2; Sd120 dump valve BV3; Sd117 dump valve BV2; Sd112 dump valve BV2; and the minimum film boiling heat transfer - qmfbsc.

The sub-optimal values of the model parameters found at this step are used as seed values for the global search. The global optimization was performed using aa number of algorithms including genetic algorithm, pattern search, simulated anneal-

ing, and particle swarm. An example of convergence of the global search for the optimal values of 14 model parameters using genetic algorithm is shown in Fig. 1.

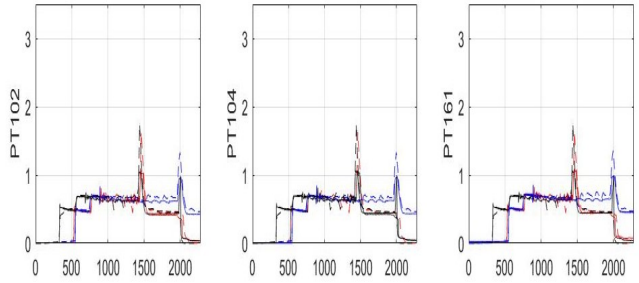

Figure 6. Comparison of the model predictions for the pressure time-series data (colored dashed lines) with the experimental results (colored solid lines) for the different openings of the valve cv112: (i) 15% blue line; (ii) 25% black line (nominal); (iii) 40% red line.

At the final step of the analysis we estimate the variance of the optimized model parameters using local search with multiple restarts. This completes the analysis of the updated distributions of the model parameters given experimental time-series data within a general inferential framework.

This procedure can be systematically continued as soon as new experimental data become available. Furthermore, alternative functional forms of the two-phase flow correlations can be compared with each other using proposed framework and available experimental databases.

The proposed approach is flexible and allows one to impose sufficient number of constraints to guarantee physically valid solution of the optimization problem.

To verify the predictions capabilities of the approach we performed the following tests. We modify in the experiment one of the control parameters while keeping all other controls at the fixed values corresponding to the nominal chilldown regime considered in the previous section. To make predictions we keep the model parameters unchanged except the one modified in the experiment.

The results of model predictions are compared with the experimental time-series in the Figs. 5 and 6. In this particular set of test measurements the opening of the control valve CV112 (BV1) was 15% (record 0056) and 40% (record 0057) as compared to the nominal opening 25 % (record 0058).

It can be seen from the figures that the system pressure is accurately reproduced for all the time-series data. The model predictions for the fluid temperature are less accurate, but are still very close to the time-traces observed in the experiment.

6. CONCLUSIONS

To summarize, we developed an efficient probabilistic framework for simultaneous optimization of a large number of correlation parameters of cryogenic loading system that enables accurate prediction of experimental time-series data. The approach relies on the fast and robust solver for two-fluid cryogenic flow reported in our earlier work.

The approach involves the following steps: (i) sensitivity analysis of the model parameters, (ii) simplified direct search for approximate globally optimal values of these parameters, (iii) global stochastic optimization that refines the estimate for parameter values obtained at the previous step, and (iv) estimation of variance of the model parameters using local non-linear optimization.

We validated this approach by analyzing chilldown in the Simulated Propellant Loading System built at NASA KSC. We perform simultaneous optimization of a large number of the model parameters. We demonstrated the convergence of the algorithm towards experimental data at the two main steps of optimization and validate its capability to predict "unseen" experimental time-traces.

We note that the proposed approach paves the way to the development of autonomous control and fault management of cryogenic two-phase flows in the future space missions.

ACKNOWLEDGMENT

This work was supported by the Advanced Exploration Systems and Game Changing Development programs at NASA HQ.

NOMENCLATURE

u	velocity
T	temperature
p	pressure
e	specific energy
h	specific enthalpy
H	heat transfer coefficient
g	gravity
Re	Reynolds number
Gr	Grashof number
Pr	Prandtl number
t	time
Δt	time step
A	cross-sectional area
S	wall surface area
V	volume of the control volume
l	perimeter
x	coordinate along the pipe
y	height of the control volume
$\dot{q}$	heat flux
c	specific heat

Greek	
α	gas void fraction
ρ	density
τ	wall shear stress
Γ	mass flux per unit volume
Subscript	
g	gas
l	liquid
w	wall
i	interface

REFERENCES

Berenson, P. (1961). Film-boiling heat transfer from a horizontal surface. *Journal of Heat Transfer*, *83*, 351–358.

Brennan, J. A., Brentari, E. G., & Smith, W. G., R. V.and Steward. (1966). *Cooldown of cryogenic transfer lines* (Technical Report No. NBS Report 9264). National Bureau of Standards.

Carbajo, J. J. (1985). A study on the rewetting temperature [Journal Article]. *Nuclear Engineering and Design*, *84*(1), 21-52.

Chato, D. J. (2008). Cryogenic fluid transfer for exploration. *Cryogenics*, *48*(5-6), 206–209.

Chung, J. N., & Yuan, K. (2015). Recent Progress on Experimental Research of Cryogenic Transport Line Chilldown Process. *Frontiers in Heat and Mass Transfer*, *6*.

Crowley, C. J., & Izenson, M. (1989). *Design manual for microgravity two-phase flow and heat transfer (u)* (Technical Report No. AL-TR-89-027). Air Force Astronautics Laboratory.

Cullimore, B. A. (1998). Optimization and automated data correlation in the nasa standard thermal/fluid system analyzer. In *Proceedings 33rd intersociety engineering conference on energy conversion.*

Darr, S., Dong, J., Glikin, N., Hartwig, J., Majumdar, A., Leclair, A., & Chung, J. (2016, oct). The effect of reduced gravity on cryogenic nitrogen boiling and pipe chilldown. *Npj Microgravity*, *2*, 16033.

Darr, S. R., Hu, H., Glikin, N., Hartwig, J. W., Majumdar, A. K., Leclair, A. C., & Chung, J. N. (2016b, dec). An experimental study on terrestrial cryogenic tube chilldown II. Effect of flow direction with respect to gravity and new correlation set. *International Journal of Heat and Mass Transfer*, *103*, 1243–1260.

Darr, S. R., Hu, H., Glikin, N. G., Hartwig, J. W., Majumdar, A. K., Leclair, A. C., & Chung, J. N. (2016a, dec). An experimental study on terrestrial cryogenic transfer line chilldown I. Effect of mass flux, equilibrium quality, and inlet subcooling. *International Journal of Heat and Mass Transfer*, *103*, 1225–1242.

Darr, S. R., Hu, H., Shaeffer, R., Chung, J., Hartwig, J. W., & Majumdar, A. K. (2015). Numerical simulation of the liquid nitrogen chilldown of a vertical tube [Book Section]. In *53rd aiaa aerospace sciences meeting.* American Institute of Aeronautics and Astronautics.

Duggento, A., Luchinsky, D. G., Smelyanskiy, V. N., & McClintock, P. V. E. (2009). Inferential framework for non-stationary dynamics: theory and applications. *Journal of Statistical Mechanics-Theory and Experiment*.

Faghri, A., & Zhang, Y. (2006). *Transport phenomena in multiphase systems* [Book]. Elsevier Science.

Franchello, G. (1993). *Development of a heat transfer package applicable to a large variety of fluids* (Scientific and Technical Research Reports No. EUR 14985 EN). European Commission.

Frost, W., & Dzakowic, G. S. (1967). An extension of the method for predicting incipient boiling on commercially finished surfaces. *ASME*, 67-HT-61.

Ghahramani, Z. (2015). Probabilistic machine learning and artificial intelligence. *Nature*, *521*(7553), 452–459.

Ghiaasiaan, S. (2007). *Two-phase flow, boiling, and condensation: In conventional and miniature systems* [Book]. Cambridge University Press.

Griffith, P. (1957). *The correlation of nucleate boiling burnout data* (Report No. NS-035-267). Massachusetts Institute of Technology.

Groeneveld, D. C., & Rousseau, J. C. (1983). Chf and post-chf heat transfer : An assessment of prediction methods and recommendations for reactor safety codes [Book Section]. In S. Kakaç & M. Ishii (Eds.), *Advances in two-phase flow and heat transfer* (Vol. 63, p. 203-237). Springer Netherlands.

Hartwig, J. W., & Vera, J. (2015, jun). Numerical Modeling of the Transient Chilldown Process of a Cryogenic Propellant Transfer Line. In *53rd aiaa aerospace sciences meeting.* American Institute of Aeronautics and Astronautics.

Hedayatpour, A., Antar, B., & Kawaji, M. (1990, jul). Analytical and numerical investigation of cryogenic transfer line chilldown. In *26th joint propulsion conference.* American Institute of Aeronautics and Astronautics.

Holman, J. P. (1989). *Heat transfer* [Book]. McGraw-Hill.

Huang, L. (2009). Evaluation of onset of nucleate boiling models. In *Eci international conference on boiling heat transfer* (Vol. 40, p. 40079216). INUS.

Iloeje, O. C., Plummer, D. N., Rohsenow, W. M., & Griffith, P. (1982). Effects of mass flux, flow quality, thermal and surface properties of materials on rewet of dispersed flow film boiling [Journal Article]. *Journal of Heat Transfer*, *104*(2), 304-308. (10.1115/1.3245088)

Jackson, J. K. (2006). *Cryogenic two-phase flow during chilldown: Flow transition and nucelate boiling heat transfer* (PhD Thesis). University of Florida.

Johnson, R., Notardonato, W., Currin, K., & Orozco-Smith, E. (2012, may). Integrated Ground Operations Demon-

stration Units Testing Plans and Status. In *Aiaa space 2012 conference & exposition.* American Institute of Aeronautics and Astronautics.

Kawaji, M. (1996, jun). Boiling heat transfer during quenching under microgravity. In *Fluid dynamics conference.* American Institute of Aeronautics and Astronautics.

Kim, S.-m., & Mudawar, I. (2014). Review of databases and predictive methods for heat transfer in condensing and boiling mini / micro-channel flows. *International Journal of Heat and Mass Transfer*, *77*, 627–652.

Konishi, C., & Mudawar, I. (2015a). Review of flow boiling and critical heat flux in microgravity [Journal Article]. *International Journal of Heat and Mass Transfer*, *80*, 469-493.

Konishi, C., & Mudawar, I. (2015b). Review of flow boiling and critical heat flux in microgravity. *International Journal of Heat and Mass Transfer*, *80*, 469–493.

Kutateladze, S. S. (1959). Critical heat flux to flowing, wetting, subcooled liquids. *Energetika*, *2*, 229–239.

Lemmon, E. W., Huber, M. L., & McLinden, M. O. (2013). *NIST Standard Reference Database 23: Reference Fluid Thermodynamic and Transport properties-REFPROP, Version 9.1, National Institute of Standards and Technology.* Retrieved from `https://www.nist.gov/srd/refprop`

Luchinskiy, D. G., Ponizovskaya-Devine, E., Hafiychuk, V., Kashani, A., Khasin, M., Timucin, D., ... Brown, B. (2015). Hierarchy of two-phase flow models for autonomous control of cryogenic loading operation [Journal Article]. *IOP Conference Series: Materials Science and Engineering*, *101*(1), 012069.

Luchinskiy, D. G., Ponizovskaya-Devine, E., Khasin, M., Timucin, D., Sass, J., Perotti, J., & Brown, B. (2015). Hierarchy of two-phase flow models for autonomous control of cryogenic loading operation. *IOP Conference Series: Materials Science and Engineering*, *101*(1), 012069.

Luchinsky, D., Khasin, M., Timucin, D., Sass, J., & Brown, B. (2016, December). Inferential framework for two-fluid model of cryogenic chilldown. *ArXiv e-prints*.

Luchinsky, D. G., Khasin, M., Timucin, D., Sass, J., Johnson, R. G., Perotti, J., & Brown, B. (2016). *Physics based model for cryogenic chilldown and loading. part iii: Correlations* (NASA/TM-2016-219093 No. NASA/TP-2016). NASA, ARC.

Luchinsky, D. G., Ponizovskaya-Devine, E., Khasin, M., Kodali, A., Perotti, J., Sass, J., & Brown, B. (2015, jan). Two-phase flow modelling of the cryogenic propellant loading system. In *51st aiaa/sae/asee joint propulsion conference* (p. 4214). American Institute of Aeronautics and Astronautics.

Luchinsky, D. G., Smelyanskiy, V. N., & Brown, B. (2014a). *Physics based model for cryogenic chilldown and loading. part i: Algorithm* (Technical Publication No. NASA/TP-2014-216659). NASA, ARC.

Luchinsky, D. G., Smelyanskiy, V. N., & Brown, B. (2014b). *Physics based model for cryogenic chilldown and loading. part ii: verification and validation* (NASA/TP-2014-218298 No. NASA/TP-2014). NASA, ARC.

Luchinsky, D. G., Smelyanskiy, V. N., & Brown, B. (2014c). *Physics based model for cryogenic chilldown and loading. part iv: Code structure* (Technical Publication No. NASA/TP-2014-218399). NASA, ARC.

Majumdar, A., & Steadman, T. (2003, jul). Numerical Modeling of Thermofluid Transients During Chilldown of Cryogenic Transfer Lines. In *33rd international conference on environmental systems* (Vol. 3). Vancouver, B.C.: Society of Automotive Engineers.

Majumdar, A. K., & Ravindran, S. S. (2010). Fast, nonlinear network flow solvers for fluid and thermal transient analysis. *International Journal of Numerical Methods for Heat & Fluid Flow*, *20*(6-7), 617–637.

Nellis, G., & Klein, S. (2009). *Heat transfer* [Book]. Cambridge University Press.

Notardonato, W. (2012, jun). Active control of cryogenic propellants in space. *Cryogenics*, *52*(46), 236–242.

RELAP5-3D-I. (2012). Code manual volume I: Code structure, system models, and solution methods [Computer software manual].

RELAP5-3D-IV. (2012). Code manual volume IV: Models and correlations (Computer software manual No. INEEL-EXT-98-00834).

Sato, T., & Matsumura, H. (1964). On the conditions of incipient subcooled-boiling with forced convection. *Bulletin of JSME*, *7*(26), 392-398.

Seader, J. D., Miller, W. S., , & Kalvinskas, L. A. (1965). *Boiling heat transfer for cryogenics* (NASA Technical Report No. NASA CR-243).

Shahs, M. M. (2006, oct). Evaluation of General Correlations for Heat Transfer During Boiling of Saturated Liquids in Tubes and Annuli. *HVAC&R Research*, *12*(4), 1047–1063.

Smelyanskiy, V. N., Luchinsky, D. G., Millonas, M. M., & McClintock, P. V. E. (2009). Recovering 'lost' information in the presence of noise: application to rodent-predator dynamics. *New Journal of Physics*, *11*.

Theler, G., & Freis, D. (2011). Theoretical critical heat flux prediction based on non-equilibrium thermodynamics considerations of the subcooled boiling phenomenon. In O. Möller, J. W. Signorelli, & M. A. Storti (Eds.), *Mecnica computacional* (Vol. XXX, p. 1713-1732).

Tong, L. S., & Tang, Y. S. (1997). *Boiling heat transfer and two-phase flow* [Book]. Taylor & Francis.

TRACE-V5.0. (2007). Theory manual field equations, solution methods, and physical models [Computer software manual].

Wojtan, L., Ursenbacher, T., & Thome, J. R. (2005). Investigation of flow boiling in horizontal tubes: Part i - a

new diabatic two-phase flow pattern map [Journal Article]. *International Journal of Heat and Mass Transfer*, *48*(14), 2955-2969.

Yuan, K., Ji, Y., & Chung, J. N. (2007). Cryogenic chilldown process under low flow rates [Journal Article]. *International Journal of Heat and Mass Transfer*, *50*(19-20), 4011-4022. (Times Cited: 6 Yuan, Kun Ji, Yan Chung, J. N. 7)

Yuan, K., Ji, Y., & Chung, J. N. (2009). Numerical modeling of cryogenic chilldown process in terrestrial gravity and microgravity [Journal Article]. *International Journal of Heat and Fluid Flow*, *30*(1), 44-53. (Times Cited: 3 Yuan, Kun Ji, Yan Chung, J. N. 4)

Zuber, N., & Tribus, M. (1958). *Further remarks on the stability of boiling* (Report No. 58-5). UCLA.

BIOGRAPHIES

Dmitry G. Luchinsky is a senior research scientist in MCT Inc. He obtained his MSc and PhD in physics in Moscow working on nonlinear optics of semiconductors. He is an author of more than 100 publications. He has been on a number of occasions a Royal Society Visiting Fellow and a NASA visiting scientist. He worked as a senior scientific researcher in VNII for Metrological Service (Moscow, Russia) and as a Senior Research Fellow in Lancaster University (Lancaster, UK). His research interests include nonlinear optics, stochastic and chaotic nonlinear dynamics, dynamical inference, fluid dynamics, ionic motion. His research is currently focused on theory and CFD of gas dynamics and cryogenic flows.

Michael Khasin Dr Michael Khasin is a Senior Researcher in SGT Inc., working at NASA Ames Research Center. He holds B.Sc. in Physics (Honors Program), 2001, M.Sc. in physics, 2003, and PhD in chemical physics, 2008, from the Hebrew University of Jerusalem. As a postdoctoral researcher at Michigan State University, Massachusetts Institute of Technology, and University of Michigan, Michael worked on the theory of non-equilibrium systems and their control and transport in disordered system. His research interests include applied physics, nonlinear and stochastic dynamics, large fluctuations and their control in non-equilibrium systems and efficient simulation of complex dynamics. He has been an invited speaker to many international and national conferences and workshops. Currently his research is focused on the theory of heat transfer, fluid dynamics, and fluid structure interaction.

Dŏgan A. Timuçin eceived the B.S. degree from Middle East Technical University, Ankara, Turkey, in 1989, and the M.S. and Ph.D. degrees from Texas Tech University, Lubbock, TX, USA, in 1991 and 1994, respectively, all in electrical engineering. He has been with the National Aeronautics and Space Administration Ames Research Center, Mountain View, CA, USA, since 1995. He has been involved in research on holographic optical memories, quantum computing algorithms, and radiative transfer models for remote sensing, statistical physics models for air traffic control, and most recently, modeling and inference of faults in electrical wiring and interconnect systems. His current research interests include selective laser melting of metal powders and nondestructive inspection of composite structures.